Experimental and Theoretical Studies of Nonclassical d^0 Cyclopentadienyl Polyhydride Complexes of Molybdenum and Tungsten

Craig A. Bayse and Michael B. Hall*

Department of Chemistry, Texas A&M University, College Station, Texas 77843

Brett Pleune

Department of Chemistry and Biochemistry, University of Maryland, College Park, Maryland 20742

Rinaldo Poli*

Laboratoire de Synthèse et d'Electrosynthèse Organométalliques, Université de Bourgogne, Faculté des Sciences "Gabriel", 6 Boulevard Gabriel, 21100 Dijon, France

Received May 5, 1998

Low-temperature protonation of compounds $Cp^*MH_5(PMe_3)$ (M = Mo, **1**; W, **2**) by $HBF_4{\cdot}Et_2O$ in CD_2Cl_2 or $CDFCl_2$ affords the thermally unstable "hexahydride" derivatives $[Cp^*MH_6(PMe_3)]^+$ (M = Mo, **3**; W, **4**). The corresponding protonation of **1**- and **2**-d^5 affords **3**- and **4**-d^5, respectively. The $\Delta\delta$ on going from H_6 to HD_5 is small for both compounds, but positive for **3** and negative for **4**, and no isotopic perturbation of resonance (IPR) is observed. The T_{1min} at 400 MHz for $[Cp^*MH_6(PMe_3)]^+$ apparently doubles on going from Mo to W (52 ms for **3** and approximately 100 ms for **4**). Optimized geometries at the restricted Hartree−Fock (RHF) and second-order Møller−Plesset (MP2) levels and energy calculations at higher levels of theory show that these complexes are dihydrogen complexes $[Cp^*M(H_2)(H)_4(PR_3)]^+$. The theoretical determination of a dihydrogen complex is consistent with the fact that the experimental T_{1min} values lie within the expected range for dihydrogen complexes. Examination of the potential energy surface at the MP2 level gives two mechanisms for hydride motion: exchange through a "trihydrogen anion" transition state and rotation of the dihydrogen ligand about its axis. The barrier for the hydride exchange (∼4 kcal/mol) is consistent with the inability to decoalesce the proton NMR signal.

Introduction

Fluxionality in transition-metal polyhydride complexes presents a challenging problem, especially in solution-phase proton NMR studies. At high temperatures, a transition-metal polyhydride complex can have a single peak due to ligands exchanging faster than the NMR time scale. This exchange-averaged signal often can be decoalesced by reducing the temperature of the experiment until multiple signals are observed corresponding to each nonequivalent proton in the system. A study of the low-temperature limit provides the best data for the determination of structural properties in the solution phase because relaxation times (T_{1min}) and proton−deuteron coupling constants (J(H,D)) can be obtained to indicate the presence of a dihydrogen ligand and estimated M−H bond lengths and dihydrogen distances. In the worst case, the proton signal cannot be decoalesced above the freezing point of common low-temperature solvents. For these complexes, J(H,D) and T_{1min} are exchange-averaged, making reasonable determination of structural parameters difficult. For these systems, theoretical studies can be used effectively to determine the low-temperature structure and to map out the mechanism of exchange. Various groups have demonstrated the utility of ab initio calculations in determining exchange mechanisms for transition-metal polyhydrides.[1]

The protonation of polyhydride complexes has been shown, at least in some cases, to occur at one of the hydride metal bonds in some systems and to afford a coordinated dihydrogen (nonclassical) species,[2] which subsequently may or may not collapse to a polyhydride (classical) moiety depending on the electron richness of the metal. The latter is obviously possible only when there are two electrons in a metal-based orbital of suitable energy. Protonation of a d^0 complex, therefore, is limited to the formation of nonclassical products, and very few examples of this type of complex have been observed experimentally, for instance $[ReH_6(\eta^2\text{-}H_2)(PR_3)_2]^+$,[2a] $[MoH_4(\eta^2\text{-}H_2)(dppe)]^{2+}$.[3] The protonation of

(1) (a) Bayse, C. A.; Couty, M.; Hall, M. B. *J. Am. Chem. Soc.* **1996**, *118*, 8916. (b) Gusev, D. G.; Kuhlman, R. L.; Renkema, K. B.; Eisenstein, O.; Caulton, K. G. *Inorg. Chem.* **1996**, *35*, 6775. (c) Clot, E.; Leforestier, C.; Eisenstein, O.; Pélisser, M. *J. Am. Chem. Soc.* **1995**, *117*, 1797. (d) Gelabert, R.; Moreno, M.; Lluch, J. M.; Lledos, A. *Organometallics* **1997**, *16*, 3805. (e) Jarid, A.; Moreno, M.; Lledos, A.; Lluch, J.; Bertrán, J. *J. Am. Chem. Soc.* **1993**, *115*, 5861.

(2) (a) Fontaine, X. L. R.; Fowles, E. H.; Shaw, B. L. *J. Chem. Soc., Chem. Commun.* **1988**, 482. (b) Chinn, M. S.; Heinekey, D. M. *J. Am. Chem. Soc.* **1987**, *109*, 5865.

S0276-7333(98)00352-5 CCC: $15.00
Publication on Web 08/27/1998

WH_6(triphos) to form $[WH_{7-2x}(\eta^2\text{-}H_2)_x(\text{triphos})]^{+\,4}$ is another possible entry into this category if $x = 1$. These d^0 dihydrogen complexes are expected to be very labile toward the loss of dihydrogen since there are no d electrons to stabilize the interaction through d−σ^* backbonding. We report here two new entries into the chemistry of d^0 dihydrogen complexes. These complexes have been synthesized through the protonation of the classical pentahydride d^0 complexes $Cp^*MH_5(PMe_3)$ (M = Mo, **1**; W, **2**) to form the dihydrogen products $[Cp^*MH_4(\eta^2\text{-}H_2)(PMe_3)]^+$ (M = Mo, **3**; W, **4**), which have been characterized by NMR and theoretical studies of the model systems $[CpMH_6(PH_3)]^+$ (M = Mo, **3T**; W, **4T**).

Experimental Details

All manipulations were carried out under an inert atmosphere of nitrogen or argon by the use of vacuum-line, Schlenk, syringe, or drybox techniques. Solvents were dried by conventional methods and distilled under nitrogen prior to use. Deuterated solvents were dried over molecular sieves and degassed by three freeze−pump−thaw cycles prior to use. Methanol was degassed by three freeze−pump−thaw cycles prior to use. ^1H and $^{31}P\{^1H\}$ NMR measurements were made on Bruker AF200, WP200, or AM400 spectrometers; the peak positions are reported with positive shifts downfield of TMS as calculated from the residual solvent peaks (^1H) and downfield of external 85% H_3PO_4 (^{31}P). For each ^{31}P NMR spectrum a sealed capillary containing H_3PO_4 was immersed in the same NMR solvent used for the measurement, and this was used as the reference. The standard inversion−recovery-pulse (180−τ−90) sequence was used to determine T_1. Values of T_1 were obtained from the slopes of linear plots of $\ln(2I_{eq}/(I_{eq} - I_\tau))$ vs τ, where I_{eq} is the peak intensity at $\tau = \infty$. $HBF_4{\cdot}Et_2O$, $LiAlD_4$, $LiAlH_4$, and PMe_3 (Aldrich) were used without further purification. Compounds $Cp^*MH_5(PMe_3)$ (M = Mo, W) and $CDFCl_2$ were synthesized by previously described methods.[5] Compounds **1**- and **2**-d^5 were synthesized by adapting these methods from $Cp^*MCl_4(PMe_3)$ and $LiAlD_4$ followed by CH_3-OD quenching. Their NMR properties are identical to those of **1** and **2**, except for the missing hydride resonances in the ^1H NMR and the P−D coupling in the $^{31}P\{^1H\}$ NMR spectra. For **1**-d^5: ^1H NMR (C_6D_6, δ): 2.19 (s, Cp*, 15H), 1.17 (d, Me, 9H, J_{PH} = 9.6 Hz). Residual hydride resonance: <4% (mol/mol). $^{31}P\{^1H\}$ NMR (C_6D_6, δ): 12.6 (1:5:15:30:45:51:45:30:15:5:1 undecet, J_{PD} = 8.9 Hz). For **2**-d^5: ^1H NMR (C_6D_6, δ): 2.31 (s, 15H, Cp*), 1.36 (d, Me, 9H, J_{PH} = 10.0 Hz). Residual hydride resonance: <5% (mol/mol). $^{31}P\{^1H\}$ NMR (C_6D_6, δ): −19.6 (1:5:15:30:45:51:45:30:15:5:1 undecet, J_{PD} = 6.5 Hz).

Protonation of $Cp^*MoH_5(PMe_3)$ (3). To a solution of 40 mg of $Cp^*MoH_5(PMe_3)$ (0.13 mmol) in 1 mL of CD_2Cl_2 at −80 °C in an NMR tube was added 20 μL of $HBF_4{\cdot}Et_2O$ (0.15 mmol) via microsyringe. The orange-brown solution darkened and began to slowly evolve H_2. ^1H NMR (CD_2Cl_2, 193 K, δ): 2.23 (s, Cp*, 15H), 1.48 (d, Me, 9H, J_{PH} = 12.1 Hz), −3.03 (d, MoH, 6H, J_{PH} = 35.5 Hz). $^{31}P\{^1H\}$ NMR ($CDFCl_2$, 193 K, δ): 2.2 (s). H_2 evolution accelerated as the solution was warmed to 0 °C. Decomposition of **3** occurs rapidly at temperatures above −60 °C; **3** has a half-life of approximately 2 h at −80 °C.

Protonation of $Cp^*WH_5(PMe_3)$ (4). To a solution of 55 mg of $Cp^*WH_5(PMe_3)$ (0.14 mmol) in 1 mL of $CDFCl_2$ at −80 °C in an NMR tube was added 25 μL of $HBF_4{\cdot}Et_2O$ (0.19 mmol) via microsyringe. The orange solution darkened and began to slowly evolve H_2. ^1H NMR ($CDFCl_2$, 193 K, δ): 2.39 (s, Cp*, 15H), 1.66 (d, Me, 9H, J_{PH} = 16.0 Hz), −2.19 (d, WH, 6H, J_{PH} = 24.7 Hz). $^{31}P\{^1H\}$ NMR ($CDFCl_2$, 193 K, δ): −21.1 (s). $^{31}P\{^1H$-selective$\}$ NMR ($CDFCl_2$, 193 K, δ): −21.1 (septet, J_{PH} = 24.0 Hz). Decomposition of **4** occurred rapidly at temperatures above −20 °C; **4** has a half-life of approximately 24 h at −80 °C.

Protonation of $Cp^*MD_5(PMe_3)$ (M = Mo, 3-d^5; W, 4-d^5). These experiments were carried out as detailed above for the corresponding pentahydride species. The results are shown in the Results and Discussion section.

Theoretical Details

The experimental complexes were modeled by replacing the methyl groups on the phosphine and Cp* ligands with hydrogens. The carbons of the Cp ring were constrained to be planar and equidistant from the metal, but the hydrogen atoms were allowed to bend in or out of the C_5 plane. The phosphine ligand was constrained to local C_{3v} symmetry.

Calculations were performed in two basis sets designated BSI and BSII. In both of these basis sets, the carbon[6a] and phosphorus[6b] atoms were treated with effective core potentials (ECPs) and double-ζ basis sets. The basis sets for the hydrogen atoms of the Cp and phosphine ligands were double-ζ quality.[7] In BSI, the metals were represented in a double-ζ basis set with a triple-ζ representation of the d orbitals (Mo (5s5p4d)/[3s3p3d]; W (5s6p4d)/[3s3p3d]) with the relativistic ECPs[8] of Ermler and Christiansen. The (n+1)s and (n+1)p orbitals of the metals have been included in accordance with recent studies on the importance of these basis functions.[9] The hydride ligands were represented by a triple-ζ basis set (5s)/[3s].[10] BSII is identical to BSI except that polarization functions (Mo (5s5p4d1f)/[3s3p3d1f]; W (5s6p4d1f)/[3s3p3d1f]; H (5s1p)/[3s1p]) have been added to the metals and hydride ligands (Mo, ζ = 0.7, W, ζ = 0.6; H, ζ = 0.475). These exponents were optimized at the MP2 level on the RHF optimized geometry of the MoH_6 and WH_6 molecules.[11]

All geometries were optimized at the restricted Hartree−Fock (RHF)[12] and second-order Møller−Plesset (MP2)[13] level of theory with full-gradient methods. For BSI, the geometries of the equilibrium and hydride−dihydrogen exchange transition states were calculated in C_1 symmetry. The dihydrogen rotation transition state was optimized in C_s symmetry with two hydride ligands constrained to have the same dihedral angle with a carbon in the Cp ring. Since BSII contained both f functions and ECPs, geometry optimizations in this basis set were performed using a Fletcher−Powell[14] line-search algorithm in C_s symmetry. For BSI, energies were recalculated at the MP3,[12] configuration interaction truncated to single and double excitations (CISD),[15] and coupled cluster truncated to single and double excitations (CCSD).[16] Relative energies were also calculated at the MP3 level in BSII. Numerical calcula-

(3) Henderson, R. A. *J. Chem. Soc., Chem. Commun.* **1987**, 1670.
(4) Michos, D.; Luo, X.-L.; Faller, J. W.; Crabtree, R. H. *Inorg. Chem.* **1993**, *32*, 1370−1375.
(5) (a) Okuda, J.; Murray, R.; Dewan, J.; Schrock, R. *Organometallics* **1986**, *5*, 1681−1690. (b) Shin, J. H.; Parkin, G. *Polyhedron* **1994**, *13*, 1489−1493. (c) Siegel, S. S.; Anet, F. A. *J. Org. Chem.* **1988**, *53*, 2629.
(6) (a) Stevens, W. J.; Basch, H.; Krauss, M. *J. Chem. Phys.* **1984**, *81*, 6026. (b) Wadt, W. R.; Hay, P. J. *J. Chem. Phys.* **1985**, *82*, 284.
(7) Dunning, T. H. *J. Chem. Phys.* **1970**, *53*, 2823.
(8) (a) LaJohn, L. A.; Christiansen, P. A.; Ross, R. B.; Atashroo, T.; Ermler, W. C. *J. Chem. Phys.* **1987**, *87*, 2812. (b) Ross, R. B.; Powers, J. M.; Atashroo T.; Ermler, W. C.; LaJohn, L. A.; Christiansen, P. A. *J. Chem. Phys.* **1990**, *93*, 6654.
(9) (a) Couty, M.; Hall, M. B. *J. Comput. Chem.* **1996**, *17*, 1359. (b) Couty, M.; Bayse, C. A.; Hall, M. B. *J. Phys. Chem.* **1996**, *100*, 13976.
(10) Dunning, T. H. *J. Phys. Chem.* **1970**, *55*, 716.
(11) Bayse, C. A.; Hall, M. B. *Inorg. Chim. Acta* **1997**, *259*, 179.
(12) Roothaan, C. C. *Rev. Mod. Phys.* **1951**, *23*, 69.
(13) (a) Møller, C.; Plesset, M. S. *Phys. Rev.* **1936**, *46*, 618. (b) Rice, J. E.; Amos, R. D.; Handy, N. C.; Lee, T. J.; Schaefer, H. F. *J. Chem. Phys.* **1986**, *85*, 963. (c) Watts, J. D.; Dupuis, M. *J. Comput. Chem.* **1988**, *9*, 158.
(14) Press: W. H.; Teukolsky, S. A.; Vettering, W. T.; Flannery, B. P. *Numerical Recipes in FORTRAN*, 2nd ed.; Cambridge University Press: Cambridge, 1992.
(15) Saunders, V. R.; van Lenthe, J. H. *Mol. Phys.* **1983**, *48*, 923.
(16) Lee, T. J.; Rice, J. E.; Rendell, A. P. The TITAN Set of Electronic Structure Programs, 1991.

Scheme 1

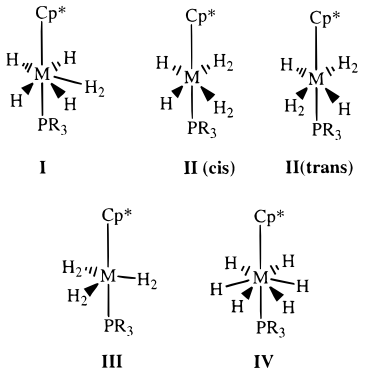

tions for the vibrational frequencies were performed at the RHF level in BSI. All calculations were performed using the GAMESS-UK package.[17]

Experimental Results

The low-temperature (−80 °C) protonation of **1** and **2** with $HBF_4{\cdot}OEt_2$ in CD_2Cl_2 or $CDFCl_2$ affords thermally unstable $[Cp^*MH_6(PMe_3)]^+$ (M = Mo, **3**; W, **4**). Complex **3** is sufficiently stable for NMR characterization only below 220 K ($t_{1/2}$ = ca. 30 s at −60 °C), whereas **4** can be investigated up to ca. 250 K ($t_{1/2}$ = ca. 2 min at −20 °C). Thermal decomposition leads to hydride-free (by NMR) uncharacterized products. The nature of the protonation products as $[Cp^*MH_6(PMe_3)]^+$ is indicated by integration of the ^1H resonance, by the absence of immediate gas evolution during the protonation reaction, and by the binomial septet pattern of the $^{31}P\{$selective-$^1H\}$ NMR resonance for **4**.

Relative to the starting pentahydride compounds, the protonation products show deshielded ^1H NMR resonances with a reduced phosphorus coupling ($\Delta\delta$ = +0.89, ΔJ_{PH} = −18.4 Hz for Mo; $\Delta\delta$ = +1.25, ΔJ_{PH} = −16.0 Hz for W) and shielded $^{31}P\{^1H\}$ NMR resonances ($\Delta\delta$ = −8.1 for Mo, −0.2 for W). The thermal instability has hampered the growth of suitable crystals for a neutron or X-ray diffraction analysis. Given the pseudopentagonal bipyramidal structure of **1** and **2**,[5b,18] a reasonable structure for complexes **3** and **4** is **I** (Scheme 1). However, protonation could induce formation of another dihydrogen ligand,[19] as in **II**. Such an occurrence was found for the protonation of $IrH_5(PCy_3)_2$ to afford $[IrH_2(\eta^2\text{-}H_2)_2(PCy_3)]^+$.[20] This structure would be isoelectronic with known half-sandwich 18-electron derivatives of Mo(IV) and W(IV) such as $Cp^*MoH_3(PMe_3)_2$[21] and $CpWH_3(PMe_3)_2$.[22] In principle, even a tris-dihydrogen structure **III** could be adopted. This would be isoelectronic with $Cp^*MoH(PMe_3)_3$.[21] For this reason, we sought additional information on these systems via NMR spectroscopic and theoretical methods.

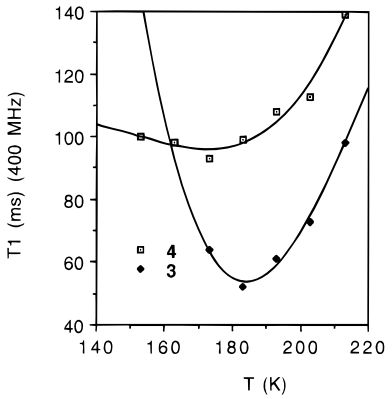

Figure 1. T_1 data for the hydride resonance of complexes $[Cp^*MH_6(PMe_3)]^+$ at 400 MHz. The solvent for **3** was CD_2Cl_2 except for the lowest temperature point ($CDFCl_2$). All of the points for **4** were done in $CDFCl_2$.

Structural information was sought experimentally by NMR through T_1 measurements,[23,24] deuteration, and isotopic perturbation of resonance (IPR) studies. The use of the T_{1min} method for the determination of polyhydride structures (e.g., classical polyhydride vs nonclassical dihydrogen complexes) is now of widespread use and provides reliable results in many cases.[19,24,25] The measured T_{1min} is 52 ms (400 MHz) at −90 °C for **3** (corresponding to 26 ms at 200 MHz; a minimum could not be reached at 200 MHz) and 51 ms (200 MHz) at −90 °C or approximately 100 ms (400 MHz) at −100 °C for **4**. The results of the T_{1min} studies at 400 MHz are graphically shown in Figure 1. Stoichiometric protonation of **1**-d^5 and **2**-d^5 with $HBF_4{\cdot}OEt_2$ in CD_2Cl_2 gave **3**- and **4**-d^5, respectively. Unfortunately, the $^{31}P\{^1H\}$, ^1H, and ^2H NMR resonances are too broad to establish the magnitude and multiplicity of the P−D and H−D couplings at all accessible temperatures. The chemical shifts of the hydride resonances of **3**(**4**)-d^5 and **3**(**4**) at different temperatures are shown in Figure 2. Given the limited temperature range of stability (especially for **3**) and the large uncertainties in $\Delta\delta = \delta(D_5H) - \delta(H_6)$ (due to broadness), the presence of IPR is not conclusively demonstrated for either compound. The detection of IPR for nonclassical complexes is often difficult.[19] It is interesting and rather unexpected, however, that the sign of $\Delta\delta$ is opposite for **3** and **4**. The replacement of H with D usually provides an upfield shift for the resonance of the residual H ligands, while a downfield shift as observed for **3** usually indicates that an IPR effect is overriding the upfield isotopic shift. Thus, although the presence of an IPR effect is not conclusively established for either compound, the result for **3** is consistent with the presence of one or more H_2 ligands as expected. The negative $\Delta\delta$ for **4** could be explained by a small IPR effect relative to the isotopic shift. A small IPR effect could result either from a small

(17) Guest, M. F.; Kendrick, J.; van Lenthe, J. H.; Schoeffel, K.; Sherwood, P. *GAMESS-UK*; Computing for Science, Ltd.: Warrington, U.K., 1995.
(18) Abugideiri, F.; Kelland, M. A.; Poli, R. *Organometallics* **1993**, *12*, 2388−2389.
(19) Crabtree, R. H. *Acc. Chem. Res.* **1990**, *23*, 95−101.
(20) Crabtree, R. H.; Hamilton, D. G. *Adv. Organomet. Chem.* **1988**, *28*, 299−338.
(21) Abugideiri, F.; Kelland, M. A.; Poli, R.; Rheingold, A. L. *Organometallics* **1992**, *11*, 1303−1311.
(22) Green, M. L. H.; Parkin, G. *J. Chem. Soc., Dalton Trans.* **1987**, 1611−1618.
(23) Calvert, R. B.; Shapley, J. R. *J. Am. Chem. Soc.* **1978**, *100*, 7726−7727.
(24) Crabtree, R. H. *The Organometallic Chemistry of the Transition Metals*, 2nd ed.; Wiley: New York, 1994.
(25) (a) Hamilton, D. G.; Crabtree, R. H. *J. Am. Chem. Soc.* **1988**, *110*, 4126−4133. (b) Cotton, F. A.; Luck, R. L. *J. Am. Chem. Soc.* **1989**, *111*, 5757−5761. (c) Luo, X.-L.; Crabtree, R. H. *Inorg. Chem.* **1990**, *29*, 2788−2791. (d) Desrosiers, P. J.; Cai, L.; Lin, Z.; Richards, R.; Halpern, J. *J. Am. Chem. Soc.* **1991**, *113*, 4173−4184. (e) Bautista, M. T.; Cappellani, E. P.; Drouin, S. D.; Morris, R. H.; Schweitzer, C. T.; Sella, A.; Zubkowski, J. *J. Am. Chem. Soc.* **1991**, *113*, 4876−4887.

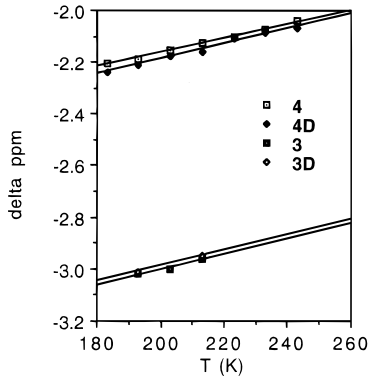

Figure 2. Temperature dependence of the chemical shift for the hydride resonance in compounds **3**, **3**-d^5 (**3D**), **4**, and **4**-d^5 (**4D**).

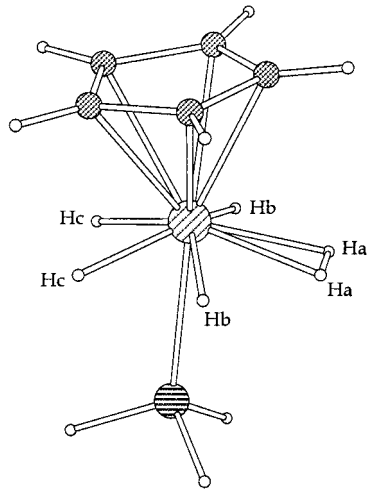

Figure 3. Geometry of $[CpW(H_2)H_4(PH_3)]^+$ at the MP2 level in BSI. Structural parameters are listed in Table 1.

difference between the chemical shifts of the hydride and dihydrogen sites or from a small zero-point energy difference between the different isotopomers. It is interesting, however, to consider the additional possibility of a symmetric σ-delocalized structure such as **IV**. Although this structure is not precedented, it would lead to the expectation of no IPR effect and an upfield shift of the NMR resonance upon deuteration. Alternatively, structure **IV** could correspond to a transition state for the hydride−dihydrogen scrambling process. However, it is more likely that a dihydrogen complex would be favored due to the electron deficient nature of the hexahydride. Additional insight into the possible structure of **3** and **4**, as well as on the mechanism of fluxionality, has been sought theoretically.

Theoretical Results

Geometry optimizations of the model complexes $[CpMH_6(PH_3)]^+$ (M = Mo, **3T**; W, **4T**) at the RHF and MP2 levels in both BSI and BSII showed that the minimum energy structure of each of these systems is the η^2-H_2 complex **I** (Figure 3). Frequency calculations in BSI at the RHF level established that these complexes are true minima on the potential energy surfaces. The geometric parameters for RHF and MP2 are very similar, and the MP2 values are listed in Table 1. Generally, both the addition of polarization functions

Table 1. Theoretical Geometries of $[CpM(H_2)H_4(PH_3)]^+$ in BSI and BSII at the MP2 Level

parameter	Mo, BSI MP2	Mo, BSII MP2	W, BSI MP2	W, BSII MP2
d(Ha−Ha), Å	0.826	0.898	0.825	0.871
d(M−Ha), Å	1.873	1.830	1.911	1.814
d(M−Hb), Å	1.732	1.709	1.735	1.706
d(M−Hc), Å	1.688	1.690	1.709	1.680
∠(X_{Cp}−M−Ha),[a] deg	100.05	102.62	100.73	102.80
∠(X_{Cp}−M−Hb),[a] deg	103.36	106.10	104.37	105.78
∠(X_{Cp}−M−Hc),[a] deg	109.40	109.56	108.22	108.69
∠(Ha−M−Ha),[a] deg	25.0	28.4	24.9	27.8
∠(C−X_{Cp}−M−Hb),[a] deg	±75.36	±76.25	±74.43	±75.21
∠(C−X_{Cp}−M−Hc),[a] deg	±143.73	±144.48	±144.25	±143.89
d(M−P), Å	2.553	2.506	2.550	2.502
d(M−C), Å	2.363	2.346	2.372	2.345
d(C−C), Å	1.474	1.476	1.473	1.475

[a] X_{Cp} is defined as the center of the Cp ring.

(BSI to BSII) and electron correlation (RHF to MP2) shorten the metal−ligand distances and lengthen the intraligand bonds (H−H and C−C distances). These polyhydride complexes have distorted pentagonal bipyramidal geometries where the hydride ligands have large bond angles with the center of the Cp ligand (X_{Cp}) of 100−109°. This distortion of the hydride ligands away from the Cp is consistent with a pseudo-second-order Jahn−Teller effect which results from the availability of low-lying unoccupied d orbitals.[26]

Calculations (MP2, BSI) were also performed on the other possible geometries **II**−**IV** for the complex with M = Mo. The bis-dihydrogen complexes reverted to **I** under full geometry optimization, but approximate structures were found by constraining the dihydrogen distances to a series of values between 0.78 and 1.14 Å. The lowest energy structures (d(H−H) = 1.02 Å) were ∼14 (cis) and ∼22 kcal/mol (trans) less stable than **I**. It was not possible to calculate the tris-dihydrogen structure **III**, as this constrained pseudo-C_{3v} system reverted to the constrained pseudo-C_{6v} hexahydride structure **IV**, which lies 19.5 kcal/mol above **I**. The addition of the f polarization functions in BSII stabilized the energy of **IV** by ∼9 kcal/mol relative to **I**. Frequency calculations on the W hexahydride structure **IV** revealed that it is a second-order saddle point on the potential energy surface (two imaginary frequencies). If structure **IV** had six equivalent M−H bonds, they would transform as $a_1+b_1+e_1+e_2$ in C_{6v} symmetry. As there is no metal orbital available of b_1 symmetry, the system is likely to be unstable. Since the available metal orbitals in **IV** ($a_1+e_1+e_2$) correspond to the bonding orbitals in C_{5v}, it is favorable for **IV** to rearrange to a geometry with five equatorial ligands: four hydrides and a dihydrogen occupying a single site.

A complex such as **I** can exchange by only one route without reduction of the metal, which is a fairly high energy process. This low-energy route (Scheme 2) involves stretching the dihydrogen toward an adjacent hydride and forming a "trihydrogen-anion ligand" at the transition state (TSE). Another transition state (TSR) for intramolecular motion involves the rotation of the dihydrogen ligand about the M−X_{H2} axis, where X_{H2} is the midpoint of the dihydrogen H−H bond.

(26) Bayse, C. A.; Hall, M. B. *Inorg. Chim. Acta* **1997**, *259*, 179, and references therein.

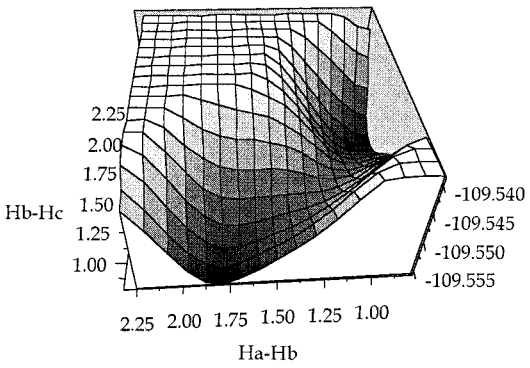

Figure 4. Potential energy surface for the exchange of hydrides in $[CpMoH_6(PH_3)]^+$ in BSI at the MP2 level.

Scheme 2

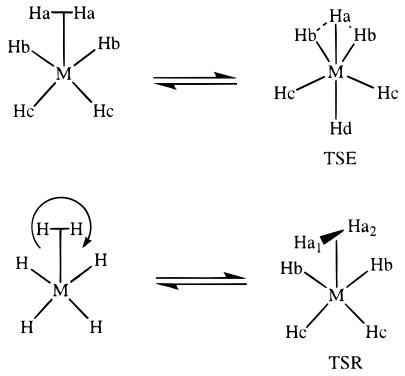

To examine the exchange mechanism in these systems, the potential energy surface (MP2, BSI) for the molybdenum complex **3T** was mapped out by constrained optimization, where the dihedral angles made by two hydride ligands, the metal, and the center of the Cp ring (X_{Cp}) to a carbon in the ring ($\angle$(H−M−X_{Cp}−C)) were fixed at various angles. Then, the surface was constructed by plotting the energy against the two smallest H−H distances from each optimization (Figure 4). An approximation to the transition state for exchange (TSE) was determined to lie at a geometry where two hydride ligands have dihedral angles ($\angle$(H−M−X_{Cp}−C)) of roughly 38°. For BSI, a Jorgensen optimization[27] was used to completely determine the exchange transition state (TSE). A similar process was used to obtain the TSE for **4T** starting from the optimized transition state for **3T**. The calculations in BSII were performed by constraining the system to C_s symmetry and performing a Fletcher−Powell[14] geometry optimization. The rotational transition state (TSR) was obtained by optimizing the geometries of the systems in C_s symmetry with equal dihedral angles ($\angle$(H−M−X_{Cp}−C)) for two hydride ligands, such that both hydrides are coplanar with a carbon in the Cp ring. Frequency calculations on TSE and TSR at the RHF level in BSI for both metal systems have one imaginary frequency, which demonstrates that these structures are true transition states. The relative energies of the transition states are shown in Table 2, and selected structural features (MP2) are shown in Figure 5 and listed in Tables 3 (TSE) and 4 (TSR).

(27) (a) Simons, J.; Jorgensen, P.; Taylor, H.; Ozment, J. *J. Phys. Chem.* **1983**, *87*, 2745. (b) Banerjee, A.; Adams, N.; Simons, J.; Shepard, R. *J. Phys. Chem.* **1985**, *89*, 52.

Table 2. Energy Barriers for Hydride Exchange in $[CpMH_6(PH_3)]^+$ Relative to $CpM(H_2)H_4(PH_3)^+$

	Mo, TSE	Mo, TSR	W, TSE	W, TSR
HF//HF[a]	11.42 (9.70)	3.09 (4.76)	10.50 (8.18)	3.96 (5.38)
MP2//MP2[a]	5.37 (2.80)	5.42 (8.45)	5.31 (2.80)	5.89 (9.32)
MP3//HF	7.04	4.27	6.42	5.06
MP3//MP2	7.39 (4.13)	4.20 (6.42)	6.95 (4.02)	5.24 (8.28)
CISD//HF	8.40	4.18	7.82	4.89
CISD//MP2	8.39	4.13	8.04	5.11
CCSD//HF	6.96	4.44	4.35	3.07
CCSD//MP2	7.35	4.19	6.95	5.23

[a] Value in parentheses in the energy barrier calculated in BSII.

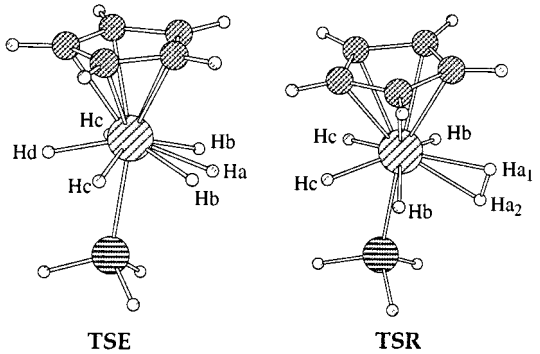

Figure 5. Geometries of TSE and TSR for $[CpW(H_2)H_4(PH_3)]^+$ at the MP2 level in BSI. Structural parameters are listed in Tables 3 and 4, respectively.

Table 3. Theoretical Geometries for the Transition State (TSE) for Hydride Exchange in BSI and BSII at the MP2 Level

parameter	Mo, BSI MP2	Mo, BSII MP2	W, BSI MP2	W, BSII MP2
d(Ha−Hb), Å	1.111	1.148	1.112	1.144
d(M−Ha), Å	1.811	1.752	1.816	1.765
d(M−Hb), Å	1.780	1.731	1.786	1.742
d(M−Hc), Å	1.724	1.700	1.723	1.695
d(M−Hd), Å	1.712	1.693	1.711	1.686
$\angle$(X_{Cp}−M−Ha),[a] deg	113.45	114.52	113.08	113.93
$\angle$(X_{Cp}−M−Hb),[a] deg	108.97	110.56	108.66	109.59
$\angle$(X_{Cp}−M−Hc),[a] deg	103.93	105.41	104.19	105.36
$\angle$(X_{Cp}−M−Hd),[a] deg	99.37	100.48	99.97	100.70
$\angle$(C−X_{Cp}−M−Hb),[a,b] deg	±38.60	±41.59	±38.31	±38.31
$\angle$(C−X_{Cp}−M−Hc),[a,b] deg	±109.18	±109.19	±109.48	±109.01
d(M−P), Å	2.552	2.505	2.553	2.509
d(M−C), Å	2.363	2.349	2.371	2.374
d(C−C), Å	1.474	1.476	1.473	1.474

[a] X_{Cp} is defined as the center of the Cp ring. [b] $\angle$(C−X_{Cp}-M-Ha) = 0.0, $\angle$(C−X_{Cp}-M-Hd) = 180.0.

At the MP2 level in BSI, the barrier to rotation is slightly higher than that for exchange, but at higher levels of electron correlation (see Table 2), the exchange barrier is 3−4 kcal/mol higher than that for rotation. In BSII, the difference in the MP2 barrier heights switches so that TSR is ∼5 kcal/mol higher than TSE. The values of the barrier height (TSE) from these calculations are consistent with the rapid exchange observed in the NMR experiment. Since the barrier heights at the MP3//MP2 and CCSD//MP2 levels give comparable results in BSI, we have calculated the barrier heights in BSII at the MP3 level. Overall, application of the larger basis set decreases the exchange barrier from ∼7 kcal/mol to ∼4 kcal/mol and increases the rotation barrier from 4 to 5 kcal/mol to 6−8 kcal/mol. The higher level calculations show that there is a slightly higher exchange barrier for **3T** (Mo)

Table 4. Theoretical Geometries for the Transition State (TSR) for Dihydrogen Rotation in BSI and BSII at the MP2 Level

parameter	Mo, BSI MP2	Mo, BSII MP2	W, BSI MP2	W, BSII MP2
$d(Ha_1-Ha_2)$, Å	0.785	0.804	0.782	0.802
$d(M-Ha_1)$, Å	1.956	1.907	1.990	1.910
$d(M-Ha_2)$, Å	1.969	1.895	1.983	1.900
d(M−Hb), Å	1.731	1.705	1.734	1.707
d(M−Hc), Å	1.710	1.681	1.706	1.679
$\angle(X_{Cp}-M-Ha_1)$,[a] deg	99.55	99.16	97.86	97.07
$\angle(X_{Cp}-M-Ha_2)$,[a] deg	122.62	123.57	120.55	121.39
$\angle(X_{Cp}-M-Hb)$,[a] deg	106.53	107.61	107.34	108.18
$\angle(X_{Cp}-M-Hc)$,[a] deg	98.59	98.55	98.57	98.63
$\angle(Ha_1-M-Ha_2)$, deg	23.0	24.4	22.7	24.3
$\angle(C-X_{Cp}-M-Hb)$,[a] deg	±78.77	±80.53	±78.29	±79.65
$\angle(C-X_{Cp}-M-Hc)$,[a] deg	±145.23	±145.58	±145.79	±145.82
d(M−P), Å	2.550	2.508	2.547	2.501
d(M−C), Å	2.362	2.340	2.375	2.340
d(C−C), Å	1.475	1.477	1.474	1.476

[a] X_{Cp} is defined as the center of the Cp ring.

and a slightly higher rotation barrier for **4T** (W), but these differences (~1 kcal/mol) are not large enough to explain the differences observed experimentally. Since the rotational barrier is probably larger than the barrier for molecular tumbling in solution,[1b] the dihydrogen ligand in the complex should not be considered to be rapidly rotating for the purpose of applying the T_{1min} criterion. Often rapidly rotating dihydrogen ligands are observed in d^4 or d^6 complexes where the occupied d orbitals provide a cylindrical area of electron density which facilitates the rapid rotation since two occupied quasi-degenerate (depending on the complex) metal orbitals can back-bond to the σ^* orbital of the dihydrogen.[1b] The d^0 complexes in this study lack this electron density (and thus lack any d → s* donor effects), a situation that results in a particularly strong cis-effect[28] in which the dihydrogen ligand is attracted to the cis hydride ligands. Thus, their rotational barriers are 2−4 times that observed for complexes with occupied d orbitals.

Discussion

The measurements of the dihydrogen distances by various methods are often inconsistent. For example, work performed on $W(H_2)(CO)_3(P^iPr_3)_2$ gives the following H−H distances: 0.75 Å (X-ray diffraction[29]), 0.82 Å (uncorrected neutron diffraction[29]), 0.89 Å (solid-state NMR[30]), 0.96 Å (solution-phase NMR[31]), 0.76 Å (solution-phase NMR with rapid rotation correction[31]), 0.85 Å (solution phase J(H,D)[32]), 0.87 Å (MP2-optimized geometry of $W(H_2)(CO)_3(PH_3)_2$[33]). X-ray diffraction is a poor method for the determination of any transition-metal hydride complex, as the hydride ligands can easily be lost in the electron density around the metal center. Neutron diffraction, on the other hand, can locate the hydrides easily, but the librational motion of a dihydrogen ligand may result in a shortened d(H−H). The solid-state NMR value is considered by some groups to be better than neutron diffraction values that have not been corrected for the librational motion of the dihydrogen ligand.[34] The librational correction lengthens the uncorrected neutron diffraction value by about 0.07 Å such that the corrected neutron diffraction value is in agreement with the solid-state NMR value. The MP2 theoretical value is in good agreement with the most accurate experimental methods.

However, the poor correlation of the solution-phase d(H−H) values calculated from T_{1min} should be noted. The inverse of T_{1min} ($1/T_{1min}$) is the sum of the effect of the different relaxation rates upon the nucleus under question.[35] For this reason, Derosiers et al.[25d] proposed including dipolar relaxations from all necessary nuclei as a correction to Crabtree's original formulation. However, while this correction gives overall good results for classical polyhydride (>3 H's) complexes, the agreement for nonclassical polyhydrides is not as good. In general, the T_{1min} method for determining dihydrogen distances is most reliable for cases where the only M−H interaction is a single dihydrogen ligand[34] (error = ±0.1 Å). In these cases, it is possible to obtain reasonable results if one accounts for librational motion and "hopping" between sites.[32] In fact, transition-metal polyhydride complexes with both nonclassical and classical hydrides in rapid exchange can be the most difficult to determine if the resonances of the nonequivalent hydride or dihydrogen ligands cannot be decoalesced. In these cases the T_{1min} value is exchange-averaged and a dihydrogen distance can only be estimated by using classical hydride structural parameters obtained from other methods. This procedure is also not necessarily reliable; for example, a recent study of $[Cp^*Os(H_2)(H)_2(PPh_3)]^+$ gave a dihydrogen distance of 1.014 Å from neutron diffraction and 1.07−1.38 Å from T_{1min}.[36] The problems in applying the T_{1min} method to several rhenium polyhydride complexes should also be noted.[25b,37]

Another method for the determination of the dihydrogen bond distance in solution is the magnitude of the proton−deuteron coupling constant J(H,D). It was observed that classical hydrides had small values (J(H,D) < 5 Hz), while dihydrogen complexes had values of 20−30 Hz. A study of a large number of complexes resulted in the following relationship between J(H,D) and the dihydrogen bond distance:

$$d(H-H) = 1.42 - 0.0167J(H,D)$$

However, while this method is more reliable than T_{1min}, it can have the same problems if the hydride resonances cannot be decoalesced and cannot be determined if the resonances are broad. Note that in the case of $W(H_2)(CO)_3(P^iPr_3)_2$ the dihydrogen bond distance

(28) Van Der Sluys, L. S.; Eckert, J.; Eisenstein, O.; Hall, J. H.; Huffman, J. C.; Jackson, S. A.; Koetze, T. F.; Kubas, G. J.; Vergamini, P. J.; Caulton, K. G. *J. Am. Chem. Soc.* **1990**, *112*, 4831.
(29) Kubas, G. J. *Acc. Chem. Res.* **1988**, *21*, 120.
(30) Zilm, K. W.; Merrill, R. A.; Kummer, M. W.; Kubas, G. J. *J. Am. Chem. Soc.* **1986**, *108*, 7837.
(31) Bautista, M. T.; Earl, K. A.; Maltby, P. A.; Morris, R. H.; Schweitzer, C. T.; Sella, A. *J. Am. Chem. Soc.* **1988**, *110*, 7031.
(32) Morris, R. H.; Wittebort, R. J. *Magn. Reson. Chem.* **1997**, *35*, 243.
(33) Bayse, C. A.; Hall, M. B. Unpublished data.
(34) Zilm, K. W.; Millar, J. M. *Adv. Magn. Opt. Reson.* **1990**, *15*, 163.
(35) Harris, R. K. *Nuclear Magnetic Resonance Spectroscopy*; Longman Scientific: New York, 1986.
(36) Gross, C. L.; Young, D. L.; Schultz, A. J.; Girolami, G. S. *J. Chem. Soc., Dalton Trans.* **1997**, 3081.
(37) (a) Cotton, F. A.; Luck, R. L. *Inorg. Chem.* **1989**, *28*, 8. (b) Cotton, F. A.; Luck, R. L. *Inorg. Chem.* **1989**, *28*, 2181.

calculated from J(H,D) is in agreement with the neutron diffraction, solid-state NMR, and theoretical results.

The systems discussed in this work are very problematic experimentally. They decompose almost immediately after formation and thus cannot be isolated. In the NMR experiments, the hydride signals did not decoalesce and were too broad to obtain J(H,D). The dihydrogen bond distances were estimated from Crabtree's isotopic formula[25a] and the positions of the hydride ligands in the theoretical structures. This method results in dihydrogen bond lengths of 0.89−1.14 Å (**3**) and 1.00−1.32 Å (**4**). However, the theoretical calculations do not reflect the difference in bond lengths indicated by the solution-phase studies (Mo < W) and, in fact, predict the opposite results (Mo > W). In a study[38] of the elongated dihydrogen complex $[CpRu(H_2)(dppm)]^+$, anharmonic vibrational corrections to the geometry were necessary to obtain the correct H−H distance. Without the correction, the H−H distances were calculated to be too short. The anharmonic corrections are critically important in that case because that d^6 system easily forms a dihydride. It is the low energy of the dihydride that results in the anharmonic potential energy.[38] Here, in the d^0 systems the potential is nearly harmonic because there is no low-lying all-hydride structure.

In conclusion, while the experimental and theoretical data are in good agreement for the Mo complex, the W complex gives a T_{1min} that is too long relative to the value that can be calculated from the optimized model. It is most likely that the difference between theory and experiment here stems from the approximations involved in applying the isotopic T_{1min} formula to a fluxional polyhydride/dihydrogen complex.

(38) Gelabert, R.; Moreno, M.; Lluch, J. M.; Lledos, A. *J. Am. Chem. Soc.* **1997**, *117*, 9840.

Conclusions

The protonation of the half-sandwich pentahydride complexes $[CpMH_5PMe_3]$ (Mo, **1**; W, **2**) are shown by theoretical methods to give the dihydrogen complexes $[CpMH_4(H_2)PMe_3^+]$ (Mo, **3**; W **4**). The experimental T_{1min} studies of these rare, highly unstable complexes give dihydrogen bond distances of 0.89−1.14 Å (**3**) and 1.00−1.32 Å (**4**), while the theoretical results are 0.898 Å (**3T**) and 0.871 Å (**4T**). While there may be discrepancies between the theoretical dihydrogen distances and those measured by T_{1min}, we feel that the theoretical results in this study are more accurate. The exchange transition states for these complexes correspond to the formation of stretched trihydrogen-anion species and have a barrier of ∼4 kcal/mol, which is in agreement with the inability to decoalesce the hydride signals at −140 °C.

Acknowledgment. Support for this work by the Department of Energy (Grant No. DEFG059ER14230 to R.P.) is gratefully acknowledged. We thank Prof. G. Parkin for providing the unpublished crystal coordinates of compound $(\eta\text{-}C_5Me_4Et)MoH_5(PMe_3)$. C.A.B. and M.B.H. thank the National Science Foundation (CHE-9423271) and the Robert A. Welch Foundation for support. The Texas A&M University Supercomputer Center is recognized for providing time on their machines. C.A.B. thanks the Robert A. Welch Foundation for support through a competitive university-wide graduate fellowship.

OM9803523